

# Oscillatory Flow in Pulsating Heat Pipes with Arbitrary Numbers of Turns

Yuwen Zhang\*

*New Mexico State University, Las Cruces, New Mexico 88003*

and

Amir Faghri†

*University of Connecticut, Storrs, Connecticut 06269*

**Oscillatory flow in pulsating heat pipes (PHPs) with arbitrary numbers of turns is investigated numerically. The PHP is placed vertically with the evaporator sections at the top and the condenser sections at the bottom. The governing equations, obtained by analysis of the conservation of mass, momentum, and energy of the liquid and vapor plugs, are nondimensionalized, and the problem is described by eight nondimensional parameters. The numerical solution is obtained by employment of an implicit scheme. The effects of the number of turns, length of the heating and cooling sections, and charge ratio on the performance of the PHP were also investigated.**

## Nomenclature

|               |   |   |
|---------------|---|---|
| $A$           | = | dimensionless amplitude of pressure oscillation |
| $A_c$         | = | cross-sectional area of the tube, $m^2$         |
| $B$           | = | dimensionless amplitude of displacement         |
| $C$           | = | integration constant                            |
| $c_p$         | = | specific heat at constant pressure, $J/kgK$     |
| $c_v$         | = | specific heat at constant volume, $J/kgK$       |
| $d$           | = | diameter of the heat pipe, $m$                  |
| $g$           | = | gravitational acceleration, $m/s^2$             |
| $H$           | = | dimensionless heat transfer coefficient         |
| $h$           | = | heat transfer coefficient, $W/m^2K$             |
| $h_{fg}$      | = | latent heat of vaporization, $J/kg$             |
| $L$           | = | length, $m$                                     |
| $L^*$         | = | dimensionless length                            |
| $M$           | = | dimensionless mass of vapor plugs               |
| $m_v$         | = | mass of vapor plugs, $kg$                       |
| $n$           | = | number of turns                                 |
| $P$           | = | dimensionless vapor pressure                    |
| $p_v$         | = | vapor pressure, $Pa$                            |
| $p^*$         | = | dimensionless parameter defined by Eq. (22)     |
| $R_g$         | = | gas constant, $J/kgK$                           |
| $T$           | = | temperature, $K$                                |
| $t$           | = | time, $s$                                       |
| $X$           | = | dimensionless displacement of liquid slug       |
| $x$           | = | displacement of liquid slug, $m$                |
| $\gamma$      | = | ratio of specific heats                         |
| $\varepsilon$ | = | charge ratio                                    |
| $\Theta$      | = | dimensionless temperature difference            |
| $\theta$      | = | dimensionless temperature                       |
| $\nu_e$       | = | effective viscosity, $m^2/s$                    |
| $\rho$        | = | density, $kg/m^3$                               |
| $\tau$        | = | dimensionless time                              |
| $\tau_p$      | = | shear stress, $N/m^2$                           |
| $\varphi$     | = | phase of oscillation                            |
| $\omega$      | = | dimensionless angular frequency                 |
| $\omega_0$    | = | dimensionless inherent angular frequency        |

## Subscripts

|     |   |                                  |
|-----|---|----------------------------------|
| $c$ | = | condenser                        |
| $e$ | = | evaporator                       |
| $h$ | = | heating                          |
| $i$ | = | $i$ th liquid slug or vapor plug |
| $L$ | = | left                             |
| $p$ | = | plug                             |
| $R$ | = | right                            |
| $v$ | = | vapor                            |

## Introduction

**P**ULSATING heat pipes (PHPs) are made from long capillary tubes bent into many turns, with the evaporator and condenser sections located at these turns.<sup>1</sup> The unique feature of PHPs, compared with the conventional heat pipe,<sup>2</sup> is that there is no wick structure to return the condensate to the heating section. Therefore, there is no countercurrent flow between the liquid and vapor. PHPs can be applied in a wide range of practical problems, including electronics cooling.<sup>3</sup> Gi et al.<sup>4</sup> investigated an O-shaped oscillating heat pipe as it applied to cooling a CPU of a notebook computer. Because of the simplicity of the PHP structure, its weight will be lower than that of a conventional heat pipe, which makes PHPs ideal candidates for space applications.

Since the PHP was invented in the early 1990s, limited experimental and analytical/numerical investigations on PHPs have been reported. The experiments mainly focused on some preliminary results for visualization of flow patterns and measurement of temperature and effective thermal conductivity. Miyazaki and Akachi<sup>5</sup> presented an experimental investigation of heat transfer characteristics of a looped PHP. They found that heat transfer limitations that usually exist in traditional heat pipes were not encountered in the PHP. The test results suggested that pressure oscillation and the oscillatory flow excite each other. A simple analytical model of self-excited oscillation was proposed based on the oscillating feature observed in the experiments. Miyazaki and Akachi<sup>6</sup> derived the wave equation of pressure oscillation in a PHP based on self-excited oscillation, in which reciprocal excitation between pressure oscillation and void fraction is assumed. They also obtained a closed-form solution of wave propagation velocity by solving the wave equation. Miyazaki and Arikawa<sup>7</sup> presented an experimental investigation on the oscillatory flow in the PHP, and they measured wave velocity, which agreed reasonably well with the prediction of Akachi et al.<sup>3</sup>

Lee et al.<sup>8</sup> reported that the oscillations of bubbles are caused by nucleate boiling and vapor oscillation, and the departure of small bubbles is considered to be the representative flow pattern at the evaporator and adiabatic section, respectively. Hosoda et al.<sup>9</sup>

Received 22 April 2002; revision received 30 November 2002; accepted for publication 28 January 2003. Copyright © 2003 by the American Institute of Aeronautics and Astronautics, Inc. All rights reserved. Copies of this paper may be made for personal or internal use, on condition that the copier pay the \$10.00 per-copy fee to the Copyright Clearance Center, Inc., 222 Rosewood Drive, Danvers, MA 01923; include the code 0887-8722/03 \$10.00 in correspondence with the CCC.

\*Assistant Professor, Department of Mechanical Engineering, Senior Member AIAA.

†Professor and Dean, School of Engineering, Associate Fellow AIAA.

investigated propagation phenomena of vapor plugs in a meandering closed-loop heat transport device. They observed a simple flow pattern appearing at high liquid volume fractions. In such conditions, only two vapor plugs exist separately in adjacent turns, and one of them starts to shrink when the other starts to grow. A simplified numerical solution was also performed with several major assumptions, including neglecting liquid film that may exist between the tube wall and a vapor plug. Shafii et al.<sup>10</sup> presented thermal modeling of a vertically placed unlooped and looped PHP with three heating sections and two cooling sections. The dimensional governing equations were solved using an explicit scheme. They concluded that the number of vapor plugs is always reduced to the number of heating sections, no matter how many vapor slugs were initially in the PHP. Zhang and Faghri<sup>11</sup> numerically investigated oscillatory flow and heat transfer in a U-shaped miniature channel. The two sealed ends of the U-shaped channel were the heating sections. The condenser section was located in the middle of the U-shaped channel. The U-shaped channel was placed vertically with two sealed ends (heating sections) at the top. The effects of various nondimensional parameters on the performance of the PHP were also investigated. The empirical correlations of amplitude and circular frequency of oscillation were obtained. Zhang and Faghri<sup>12</sup> proposed heat transfer models in the evaporator and condenser sections of a PHP with one open end by analysis of thin-film evaporation and condensation. The heat transfer solutions were applied to the thermal model of the PHP, and a parametric study was performed. Both Shafii et al.<sup>10</sup> and Zhang and Faghri<sup>12</sup> found that heat transfer in a PHP was due mainly to the exchange of sensible heat because over 90% of the heat transferred from the evaporator to the condenser is due to sensible heat. The role of evaporation and condensation on the operation of PHPs was mainly on the oscillation of liquid slugs, and the contribution of latent heat on the overall heat transfer was not significant.

In the present study, an analysis of oscillatory flow in a PHP with an arbitrary number of turns will be presented. The governing equations are first nondimensionalized, and the parameters of the system will be reduced to several dimensionless numbers. The nondimensional governing equations are then solved numerically, and the effects of various parameters on oscillatory flow in the PHP will be investigated.

### Physical Model

A schematic of the PHP under investigation is shown in Fig. 1. A tube with diameter  $d$  and length  $2nL$  is bent into  $n$  turns, with the two ends sealed. The evaporator sections of the PHP are at the upper portion, and each of them has a length of  $L_h$ . The condenser sections with length  $L_c$  are located at the lower portion of the PHP. The adiabatic sections, located between the evaporation and condenser sections, have a length of  $L_a$ . The wall temperatures at the evaporator and condenser sections are  $T_e$  and  $T_c$ , respectively. The liquid slugs with uniform length  $2L_p$  are located at the bottom of the PHP.<sup>7,10</sup> The

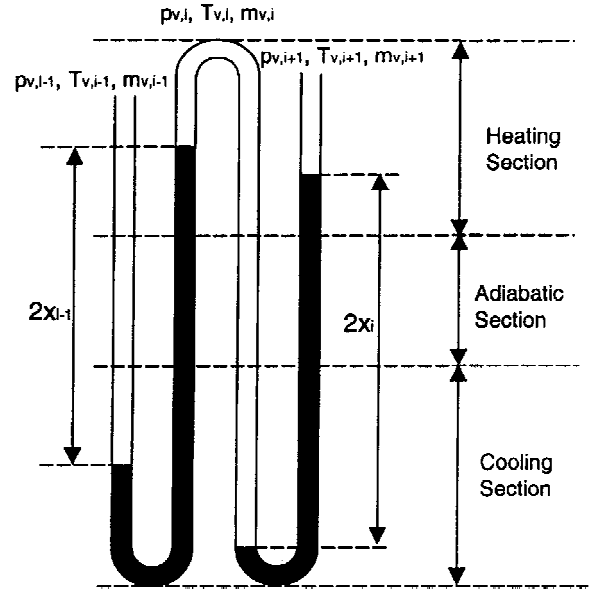


Fig. 2 Heating and cooling sections of a PHP.

location of each liquid slug can be represented by the displacement  $x_i$ , which is zero when the liquid slug is exactly in the middle of the turns. When the liquid slug shifts to the right, the displacement is positive. When the liquid slug shifts to the left, the displacement is negative. The operation of the PHP is accomplished by oscillation of the liquid slugs due to evaporation and condensation in the vapor plugs.

### Governing Equations

The momentum equation for the liquid slug in Fig. 2 can be expressed as

$$2A_c L_p \rho_l \frac{d^2 x_i}{dt^2} = (p_{v,i} - p_{v,i+1}) A_c - 2\rho_l g A_c x_i - 2\pi d L_p \tau_p \quad (1)$$

where  $A_c = \pi d^2/4$  is the cross-sectional area of the tube.

Equation (1) can be rearranged as

$$\frac{d^2 x_i}{dt^2} + \frac{32\nu_e}{d^2} \frac{dx_i}{dt} + \frac{g}{L_p} x_i = \frac{p_{v,i} - p_{v,i+1}}{2\rho_l L_p} \quad (2)$$

where  $\nu_e$  is the effective kinetic viscosity of the liquid.

The energy equation of the vapor plugs is obtained by application of the first law of thermodynamics to each plug

$$\frac{d(m_{v,i} c_v T_{v,i})}{dt} = c_p T_{v,i} \frac{dm_{v,i}}{dt} - p_v \frac{\pi d^2}{4} \left( \frac{dx_i}{dt} - \frac{dx_{i-1}}{dt} \right) \quad (3)$$

Expansion of the left-hand side of Eq. (3) yields

$$m_{v,i} c_v \frac{dT_{v,i}}{dt} + c_v T_{v,i} \frac{dm_{v,i}}{dt} = c_p T_{v,i} \frac{dm_{v,i}}{dt} - p_v \frac{\pi d^2}{4} \left( \frac{dx_i}{dt} - \frac{dx_{i-1}}{dt} \right)$$

which can be rearranged as

$$m_{v,i} c_v \frac{dT_{v,i}}{dt} = (c_p - c_v) T_{v,i} \frac{dm_{v,i}}{dt} - p_v \frac{\pi d^2}{4} \left( \frac{dx_i}{dt} - \frac{dx_{i-1}}{dt} \right)$$

If the vapor can be considered an ideal gas that satisfies  $c_p - c_v = R_g$ , the energy equation in the vapor phase becomes

$$m_{v,i} c_v \frac{dT_{v,i}}{dt} = R_g T_{v,i} \frac{dm_{v,i}}{dt} - p_v \frac{\pi d^2}{4} \left( \frac{dx_i}{dt} - \frac{dx_{i-1}}{dt} \right) \quad (4)$$

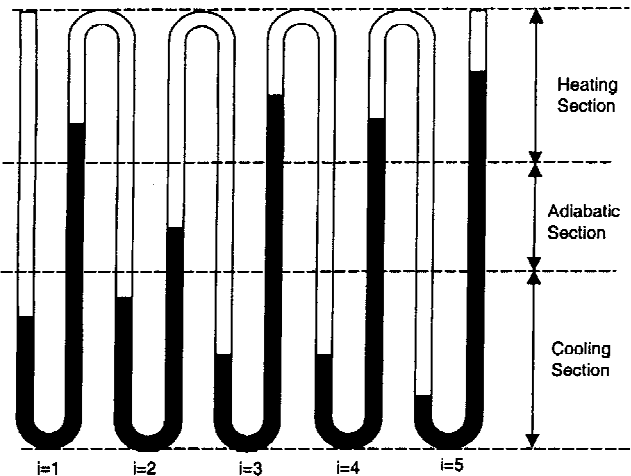


Fig. 1 PHP.

The behavior of vapor plugs in the evaporators can be modeled by the use of the ideal gas law

$$p_{v,1}[(L - L_p) + x_1](\pi/4)d^2 = m_{v,1} R_g T_{v,1} \quad (5a)$$

$$p_{v,i}[2(L - L_p) + x_i - x_{i-1}](\pi/4)d^2 = m_{v,i} R_g T_{v,i} \quad (5b)$$

$$i = 2, 3, \dots, n$$

$$p_{v,n+1}[(L - L_p) - x_n](\pi/4)d^2 = m_{v,n+1} R_g T_{v,n+1} \quad (5c)$$

When Eq. (5b) is substituted into Eq. (4) to eliminate vapor plug pressure,  $p_{v,i}$  yields

$$m_{v,i} c_v \frac{dT_{v,i}}{dt} = R T_{v,i} \frac{dm_{v,i}}{dt} - \frac{m_{v,i} R_g T_{v,i} (dx_i/dt - dx_{i-1}/dt)}{[2(L - L_p) + x_i - x_{i-1}]} \quad (6)$$

that is,

$$\frac{1}{m_{v,i}} \frac{dm_{v,i}}{dt} = \frac{1}{\gamma - 1} \frac{1}{T_{v,i}} \frac{dT_{v,i}}{dt} + \frac{(d/dt)[(2L - L_p) + x_i - x_{i-1}]}{[(2L - L_p) + x_i - x_{i-1}]} \quad (7)$$

where  $\gamma = c_p/c_v$  is the specific heat ratio of the vapor.

When Eq. (7) is integrated, a closed form of the mass of the vapor plug is obtained:

$$m_{v,i} = C_i T_{v,i}^{1/(\gamma-1)} [2(L - L_p) + x_i - x_{i-1}], \quad i = 2, 3, \dots, n \quad (8)$$

Similarly, the masses of the first and last vapor plug are

$$m_{v,1} = C_1 T_{v,1}^{1/(\gamma-1)} [(L - L_p) + x_1] \quad (8a)$$

$$m_{v,n+1} = C_{n+1} T_{v,n+1}^{1/(\gamma-1)} [(L - L_p) - x_n] \quad (8b)$$

where  $C_i$  is the integration constant. When Eqs. (8a), (8), and (8b) are substituted into Eqs. (5a–5c), the pressures of the vapor plug are

$$p_{v,i} = \frac{4C_i R_g}{\pi d^2} T_{v,i}^{\gamma/(\gamma-1)}, \quad i = 1, 2, \dots, n \quad (9)$$

The masses of the vapor plugs increase due to evaporation and decrease due to condensation

$$\frac{dm_{v,i}}{dt} = \frac{h_e \pi d (T_e - T_{v,i})(L_{h,L} + L_{h,R})}{h_{fg}} - \frac{h_c \pi d (T_{v,i} - T_c)(L_{c,L} + L_{c,R})}{h_{fg}} \quad (10)$$

where  $L_{h,L}$  and  $L_{h,R}$  are lengths of evaporator sections that are in contact with the vapor plug, and  $L_{c,L}$  and  $L_{c,R}$  are lengths of condenser sections that are in contact with the vapor plug (Fig. 2).

$$L_{h,L} = \begin{cases} L - (L_p + x_{i-1}) & L_p + x_{i-1} \geq L_c + L_a \\ 0 & L_p + x_{i-1} < L_c + L_a \end{cases} \quad (11a)$$

$$L_{h,R} = \begin{cases} L - (L_p - x_i) & L_p - x_i \geq L_c + L_a \\ 0 & L_p - x_i < L_c + L_a \end{cases} \quad (11b)$$

$$L_{c,L} = \begin{cases} L_c - (L_p + x_{i-1}) & L_p + x_{i-1} < L_c \\ 0 & L_p + x_{i-1} \geq L_c \end{cases} \quad (11c)$$

$$L_{c,R} = \begin{cases} L_c - (L_p - x_i) & L_p - x_i < L_c \\ 0 & L_p - x_i \geq L_c \end{cases} \quad (11d)$$

### Nondimensional Governing Equations

To nondimensionalize the governing equations, a reference state of the PHP needs to be specified. At this reference state, the pressure and temperature of all of the vapor plugs are  $p_0$  and  $T_0$ , respectively. The displacement of all of the liquid plugs at the reference state are  $x_i = x_0$ . According to Eq. (9), the constants  $C_i$  for different vapor plugs are the same and can be expressed as

$$C_i = C = (\pi d^2 / 4 R_g) p_0 T_0^{-(\gamma-1)/\gamma} \quad (12)$$

The masses of the vapor plugs at the reference state are

$$m_{v0,1} = \frac{\pi d^2}{4 R_g T_0} p_0 [(L - L_p) + x_0] \quad (13a)$$

$$m_{v0,i} = \frac{\pi d^2}{2 R_g T_0} p_0 (L - L_p), \quad n = 2, 3, \dots, n \quad (13b)$$

$$m_{v0,n+1} = \frac{\pi d^2}{4 R_g T_0} p_0 [(L - L_p) - x_0] \quad (13c)$$

The average mass of the first and last vapor plugs is

$$m_0 = \frac{m_{v0,1} + m_{v0,n+1}}{2} = \frac{\pi d^2}{2 R_g T_0} p_0 (L - L_p) = m_{v0,i} \quad (14)$$

Substitution of Eqs. (12) and (14) into Eqs. (8a), (8), (8b), and (9) yields

$$\frac{m_{v,1}}{m_0} = \left( \frac{T_{v,1}}{T_0} \right)^{1/\gamma} \frac{L - L_p + x_1}{2(L - L_p)} \quad (15a)$$

$$\frac{m_{v,i}}{m_0} = \left( \frac{T_{v,i}}{T_0} \right)^{1/\gamma} \frac{2(L - L_p) + x_i - x_{i-1}}{2(L - L_p)} \quad (15b)$$

$$\frac{m_{v,n+1}}{m_0} = \left( \frac{T_{v,n+1}}{T_0} \right)^{1/\gamma} \frac{L - L_p - x_n}{2(L - L_p)} \quad (15c)$$

$$\frac{p_{v,i}}{p_0} = \left( \frac{T_{v,i}}{T_0} \right)^{\gamma/(\gamma-1)} \quad (16)$$

By definition of

$$\theta_i = T_{v,i}/T_0, \quad P_i = p_{v,i}/p_0, \quad M_i = m_{v,i}/m_0$$

$$X_i = x_i/x_0, \quad \varepsilon = L_p/L \quad (17)$$

Eqs. (15) and (16) become

$$M_1 = \theta_1^{1/\gamma} \left[ \frac{1}{2} + \frac{X_1}{2(1-\varepsilon)} \right] \quad (18a)$$

$$M_i = \theta_i^{1/\gamma} \left[ 1 + \frac{X_i - X_{i-1}}{2(1-\varepsilon)} \right], \quad i = 2, 3, \dots, n \quad (18b)$$

$$M_{n+1} = \theta_{n+1}^{1/\gamma} \left[ \frac{1}{2} - \frac{X_n}{2(1-\varepsilon)} \right] \quad (18c)$$

$$P_i = \theta_i^{\gamma/(\gamma-1)}, \quad i = 1, 2, \dots, n+1 \quad (19)$$

When the nondimensional variables are introduced to Eq. (2) and dimensionless time is defined as

$$\tau = v_e t / d^2 \quad (20)$$

Eq. (2) becomes

$$\frac{d^2 X_i}{d\tau^2} + 32 \frac{dX_i}{d\tau} + \omega_0^2 X_i = p(P_i - P_{i+1}), \quad i = 1, 2, \dots, n \quad (21)$$

where  $\omega_0$  and  $p$  are two dimensionless parameters defined as

$$\omega_0^2 = \frac{g d^4}{L_p v_e^2}, \quad p = \frac{p_0 d^4}{2 \rho_\ell L_p L_h v_e^2} \quad (22)$$

Substituting Eqs. (17) and (20) into Eq. (10), one obtains

$$\begin{aligned} \frac{dM_i}{d\tau} &= H_e (L_{c,L}^* + L_{c,R}^*) (\theta_e - \theta_i) \\ &\quad - H_c (L_{c,L}^* + L_{c,R}^*) (\theta_i - \theta_c) \end{aligned} \quad (23)$$

where

$$\begin{aligned} H_c &= \frac{4 h_c R T_0^2 d}{p_0 h_{fg} v_e}, \quad H_e = \frac{4 h_e R T_0^2 d}{p_0 h_{fg} v_e} \\ \theta_c &= \frac{T_c}{T_0}, \quad \theta_e = \frac{T_e}{T_0} \end{aligned} \quad (24)$$

The dimensionless lengths of the vapor plug in the heating and cooling sections in Eq. (23) are

$$L_{h,L}^* = \frac{L_{h,L}}{L} = \begin{cases} 1 - (\varepsilon + X_{i-1}) & \varepsilon + X_{i-1} \geq 1 - L_h^* \\ 0 & \varepsilon + X_{i-1} < 1 - L_h^* \end{cases} \quad (25a)$$

$$L_{h,R}^* = \frac{L_{h,R}}{L} = \begin{cases} 1 - (\varepsilon - X_i) & \varepsilon - X_i \geq 1 - L_h^* \\ 0 & \varepsilon - X_i < 1 - L_h^* \end{cases} \quad (25b)$$

$$L_{c,L}^* = \frac{L_{c,L}}{L} = \begin{cases} L_c^* - (\varepsilon + X_{i-1}) & \varepsilon + X_{i-1} < L_c^* \\ 0 & \varepsilon + X_{i-1} \geq L_c^* \end{cases} \quad (25c)$$

$$L_{c,R}^* = \frac{L_{c,R}}{L} = \begin{cases} L_c^* - (\varepsilon - X_i) & \varepsilon - X_i < L_c^* \\ 0 & \varepsilon - X_i \geq L_c^* \end{cases} \quad (25d)$$

where

$$L_h^* = L_h/L, \quad L_c^* = L_c/L \quad (26)$$

The system is described by nine nondimensional parameters, including the number of turns  $n$ , and the parameters defined in Eqs. (22), (24), and (26). If the reference temperature is chosen to be the average of  $T_e$  and  $T_c$ , the dimensionless temperature of the heating and cooling sections is

$$\theta_e = 1 + \Theta, \quad \theta_c = 1 - \Theta \quad (27)$$

where

$$\Theta = (T_e - T_c)/(T_e + T_c) \quad (28)$$

At this point, the number of dimensionless parameters that describe the system are further reduced to eight.

### Initial Conditions

The reference state of the PHP is chosen to be the initial state of the system. The initial conditions of the system are

$$X_i = X_0, \quad \tau = 0, \quad i = 1, 2, \dots, n \quad (29)$$

$$P_i = 1, \quad \tau = 0, \quad i = 1, 2, \dots, n \quad (30)$$

$$\theta_i = 1, \quad \tau = 0, \quad i = 1, 2, \dots, n \quad (31)$$

$$M_1 = \frac{1}{2} + X_0/2(1 - \varepsilon), \quad \tau = 0 \quad (32a)$$

$$M_i = 1, \quad \tau = 0, \quad i = 2, 3, \dots, n \quad (32b)$$

$$M_{n+1} = \frac{1}{2} - X_0/2(1 - \varepsilon), \quad \tau = 0 \quad (32c)$$

### Numerical Solution

The oscillatory flow in a PHP is described by Eqs. (18), (19), (21), and (23), with initial conditions specified by Eqs. (29–32). Note that Eq. (21) is an ordinary differential equation of forced vibration. If the vapor pressure difference between the two vapor plugs at two ends of the liquid slug is

$$P_i - P_{i+1} = A_i \cos \omega_i \tau \quad (33)$$

the analytical solution of Eq. (21) can be obtained, and it will have the following form<sup>11</sup>

$$X_i = B_i \cos(\omega_i \tau - \varphi_i) \quad (34)$$

However, the amplitude and angular frequency are unknown a priori and the pressure difference between the two vapor plugs depends on heat transfer in two vapor plugs. The amplitude and angular frequency of pressure oscillation must be obtained numerically. The results of each time step are obtained when the dimensionless governing equations are solved with an implicit scheme. The numerical procedure for a particular time step is outlined as follows:

- 1) Guess the dimensionless temperatures of all vapor plugs  $\theta_i$ .
- 2) Obtain the dimensionless vapor pressure  $P_i$ , from Eq. (19).
- 3) Calculate the dimensionless displacement of liquid slug  $X_i$  from Eq. (21).
- 4) Calculate the mass of the vapor plugs  $M_i$  by the use of Eq. (23).
- 5) Calculate the nondimensional temperature of the vapor plugs  $\theta_i$  from Eqs. (18a–18c).
- 6) Compare  $\theta_i$  obtained in step 5 with the guessed values in step 1. If the differences meet a tolerance, go to the next step; otherwise, steps 2–5 are repeated until a converged solution is obtained.

The use of an implicit scheme ensured the stability of the numerical solution. To obtain a time-step independent solution, the time step was systematically varied to find the appropriate time step. The numerical results showed that the time-step independent solution can be obtained when the time step is  $\Delta\tau = 10^{-5}$  because there are no notable changes in the results when the time step is reduced from  $10^{-5}$  to  $10^{-6}$ . All results presented in the following section were obtained by the use of the time step  $\Delta\tau = 10^{-5}$ .

### Results and Discussions

Figure 3a shows the comparison of the liquid slug displacement obtained by the present model and the model of Zhang et al.<sup>11</sup> who studied oscillatory flow in a U-shaped miniature channel. The present result is obtained by the set of the number of turns,  $n = 1$ . Note that the agreement between the results obtained by the present model and Zhang et al.<sup>11</sup> is excellent. Figure 3b shows the comparison of the liquid slug displacements obtained by the present model and the model of Shafii et al.<sup>10</sup> The results of the Shafii et al. model<sup>10</sup> were obtained with the following parameters:  $L_h = 0.1$  m,  $L_a = 0$  m,  $L_c = 0.1$  m,  $L_p = 0.2$  m,  $d = 3.34$  mm,  $T_e = 123.4^\circ$  C,  $T_c = 20^\circ$  C, and  $h_e = h_c = 200$  W/m<sup>2</sup>K. The present results were obtained with the corresponding nondimensional parameters:  $\omega_0^2 = 1.2 \times 10^4$ ,  $p = 1.2 \times 10^5$ ,  $\Theta = 0.15$ ,  $H_e = H_c = 3000$ ,  $L_h^* = 0.5$ ,  $L_c^* = 0.5$ , and  $n = 2$ . Note that the results obtained with the present model agreed very well with the results obtained by the Shafii et al. model,<sup>10</sup> which employed dimensional parameters and was applicable only to PHPs with two turns. The phase of the oscillation of two vapor plugs are the same for the first several periods. Steady oscillation is established after  $\tau = 0.09$ , at which time the amplitudes of oscillation for the two liquid slugs are the same. The phase difference for the oscillation of the two liquid slugs is equal to  $\pi$ , which means that the oscillation of the liquid slug in the PHP with two turns is symmetric after steady oscillation is established. The amplitude and circular frequency for oscillation in a PHP with two turns are the same as those for a U-shaped channel. At the parameters just specified, the amplitude and circular frequency of oscillation for both  $n = 1$  and  $n = 2$  are  $B = 0.31489$  and  $\omega = 597.78$ , respectively. As indicated in the numerical simulations by Shafii et al.<sup>10</sup> and Zhang

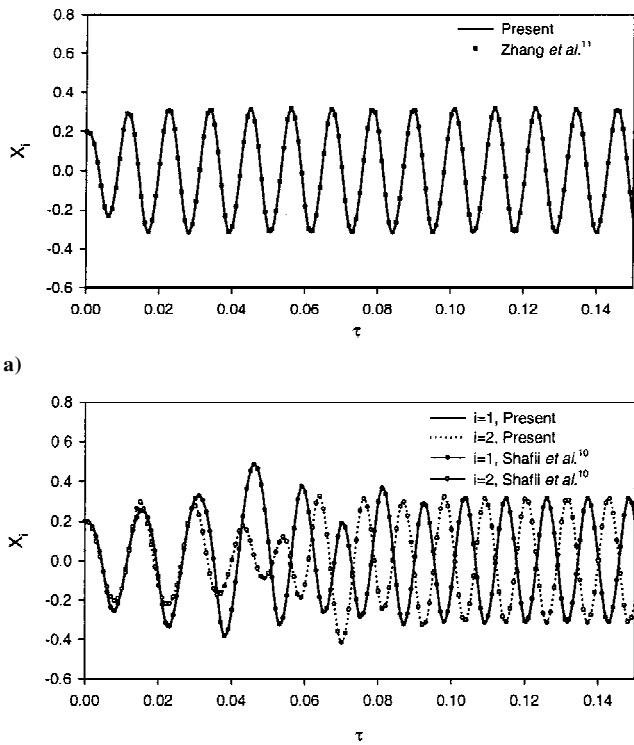


Fig. 3 Comparison of the present results with a) Zhang et al.<sup>11</sup> and b) Shafii et al.<sup>10</sup>

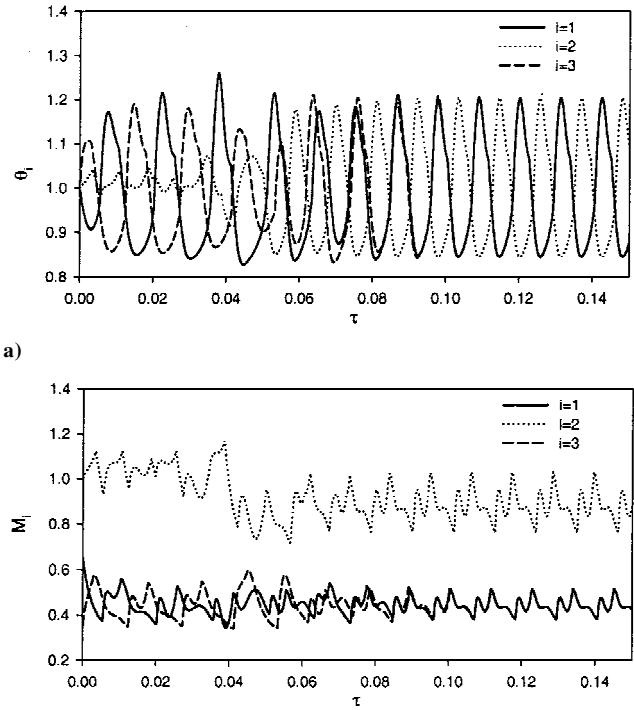


Fig. 4 Dimensionless a) temperature and b) mass of the vapor plugs ( $n = 2$ ).

and Faghri,<sup>12</sup> heat transfer in a PHP is mainly due to the exchange of sensible heat, that is, liquid slugs absorb heat in the heating sections and release heat in the cooling section of the PHP. The large amplitude of the oscillatory flow allows the liquid slug to achieve better contact with the heating and cooling sections of the PHP. On the other hand, a large circular frequency of oscillatory flow allows quicker motion of liquid slug between the heating and cooling sections of the PHP. Therefore, both large amplitude and higher circular

frequency are desirable for better heat transfer performance of the PHP.

Figure 4a shows the dimensionless temperature of three vapor plugs. The maximum temperature of the vapor plug can exceed the heating wall temperature of the PHP due to compression of the vapor plug. The variations of the dimensionless temperatures of the first and third vapor plugs become identical after steady oscillation is established at  $\tau = 0.09$ . Figure 4b shows the variation of

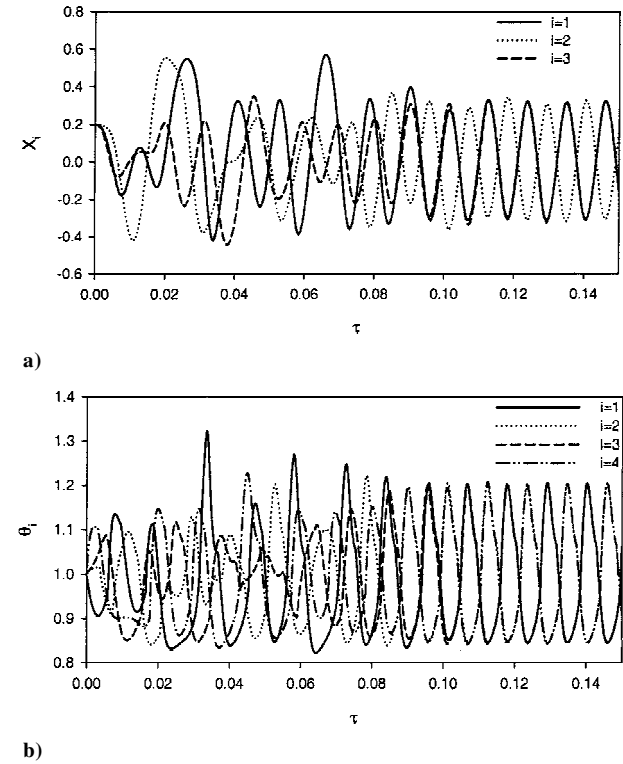


Fig. 5 Dimensionless a) displacement of liquid slugs and dimensionless b) temperature of the vapor plugs ( $n = 3$ ).

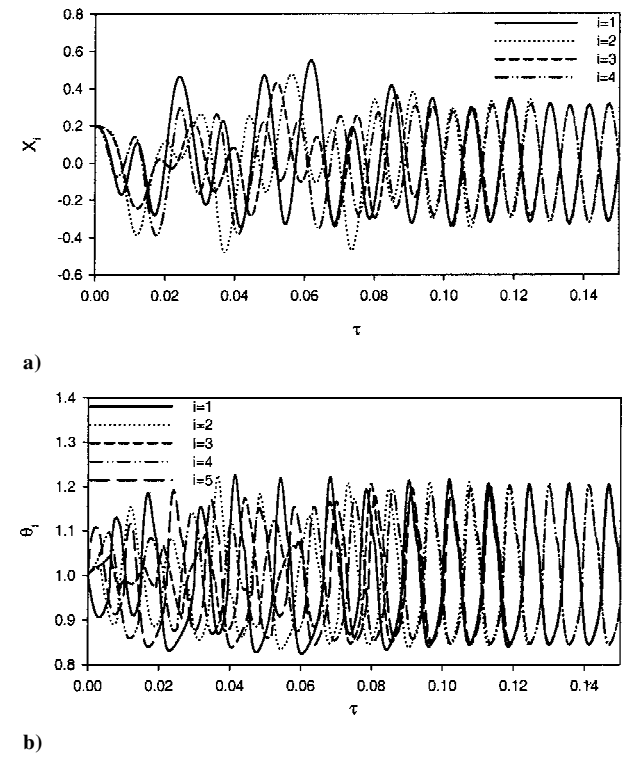


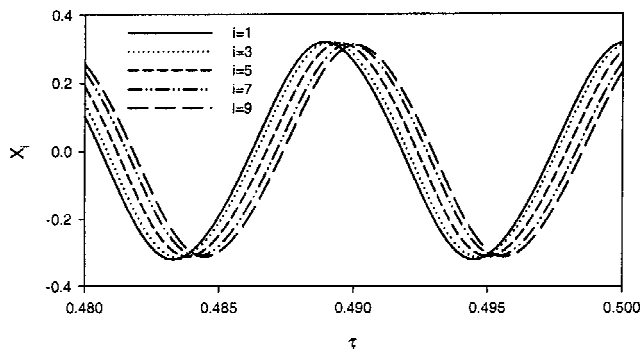
Fig. 6 Dimensionless a) displacement of liquid slugs and dimensionless b) temperature of the vapor plugs ( $n = 4$ ).

dimensionless mass of the vapor plugs. The masses of first and third vapor plugs were different at the beginning, but they are identical after steady oscillation is established. The mass of the second vapor plug is twice that of first or third vapor plugs after steady oscillation is established. The history of vapor plug temperature and mass further indicated that the oscillations in the PHP with two turns are symmetric. The differences between the oscillations in PHP with one or two turns can be observed before steady oscillation is established. After steady oscillation is established, the oscillation in the U-shaped channel is the same as that in the PHP with two turns.

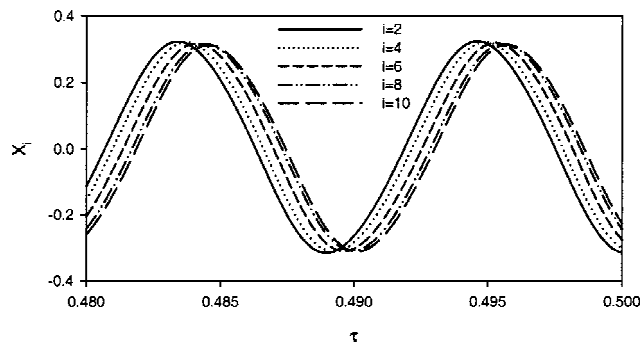
Figure 5 shows oscillatory flow in a PHP with three turns. The time required to establish steady oscillation for the PHP with three turns is longer than that for the PHP with two turns. Once steady oscillation is established, the dimensionless displacements of the first and third liquid slugs become identical, which means that the oscillation is symmetric for the PHP with three turns. Figure 5b shows the dimensionless temperatures of the vapor plugs for the PHP with three turns. The dimensionless temperatures of an odd number of vapor plugs are identical once steady oscillation is established. The dimensionless temperature of an even number of vapor plugs are also identical once steady oscillation is established, but their phase

difference with odd numbered vapor plugs is  $\pi$ . The amplitude and circular frequency of oscillation are same as those of  $n = 1$  and 2. Figure 6 shows oscillatory flow in a PHP with four turns. The time required to establish steady oscillation for the PHP with four turns is about  $\tau = 0.13$ , which is longer than that for PHP with three turns. The dimensionless displacements of the odd-numbered liquid slugs become identical once steady oscillation is established. The dimensionless displacements of the even-numbered liquid slugs are also identical after  $\tau = 0.13$ . Figure 5b shows the dimensionless temperature of the vapor plugs for the PHP with four turns. Similar to the case with three turns, the phase difference between odd- and even-numbered vapor plugs is also  $\pi$ . The increase in the number of turns from three to four did not result in any changes in the amplitude and circular frequency of oscillation.

Numerical simulations are then performed for PHPs with different numbers of turns. The results show that the amplitude and frequency of oscillation of PHPs are not affected by the number of turns until  $n = 6$ . When the number of turns is increased to 6, the amplitude and frequency of oscillation for different liquid slugs begin to differ. The

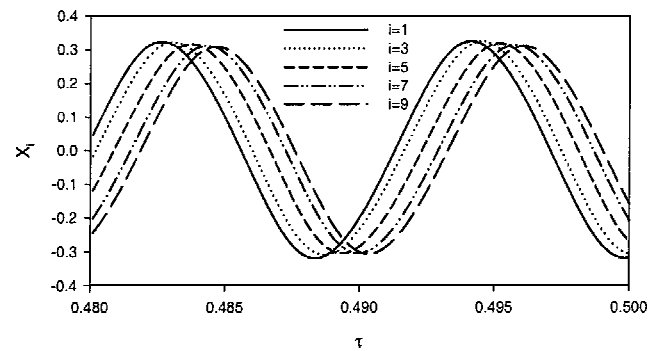


a) Odd number liquid slugs

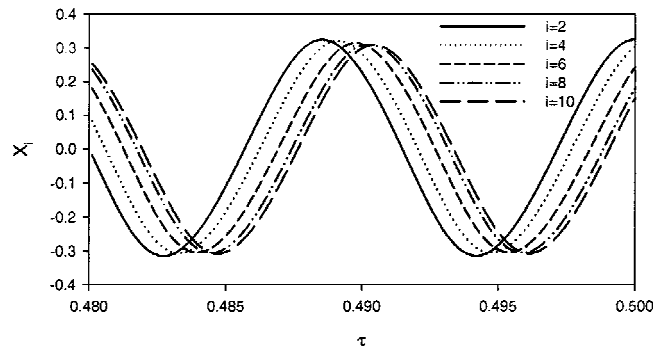


b) Even number liquid slugs

Fig. 7 Displacement of liquid slugs ( $n = 10$ ).



a) Odd number liquid slugs



b) Even number liquid slugs

Fig. 9 Displacement of liquid slugs ( $L_h^* = L_c^* = 0.45$ ).

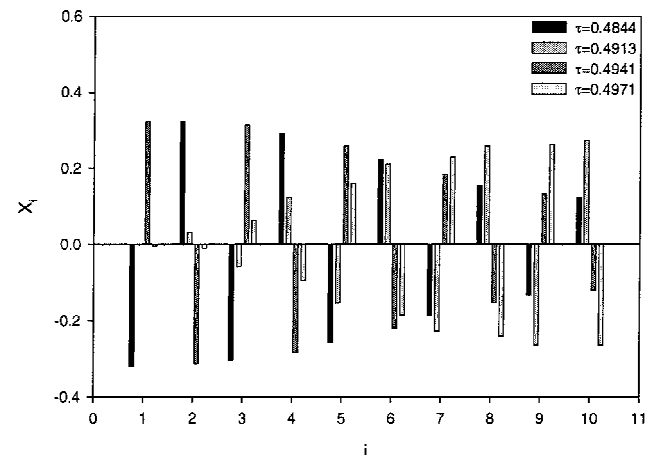


Fig. 10 Distribution of the displacement of liquid slugs ( $L_h^* = L_c^* = 0.45$ ).

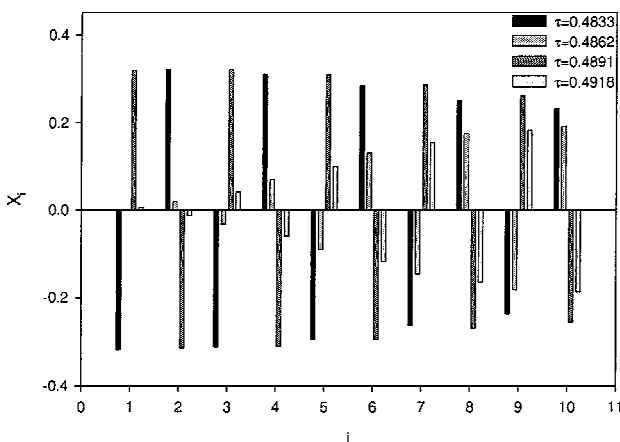
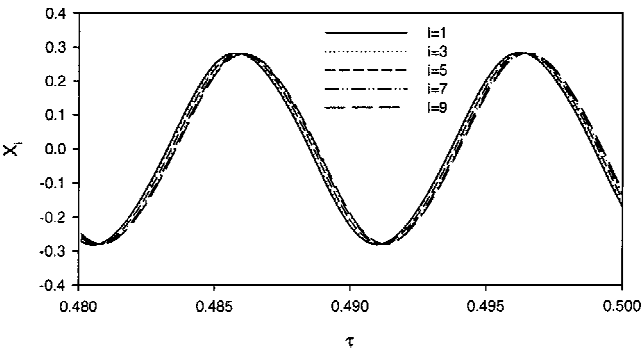


Fig. 8 Distribution of the displacement of liquid slugs ( $n = 10$ ).

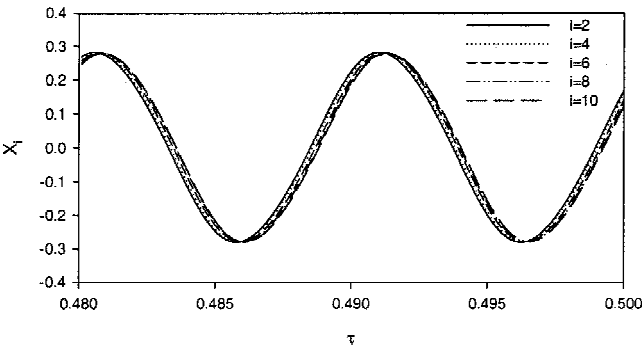
amplitude and circular frequency of oscillation for different number of turns are shown in Table 1. The amplitude and circular frequency for different liquid slugs in the same PHP are slightly different when the number of turns is greater than five. However, note that the amplitudes and circular frequencies for different turns are only very slightly different. When  $n = 10$ , the maximum differences of the amplitudes and circular frequencies for different turns are only 3 and 0.5%, respectively.

Table 1 Amplitude and circular frequency of oscillatory flow in PHPs

| <i>i</i> |          | <i>n</i> = 6 | <i>n</i> = 7 | <i>n</i> = 8 | <i>n</i> = 9 | <i>n</i> = 10 |
|----------|----------|--------------|--------------|--------------|--------------|---------------|
| 1        | <i>B</i> | 0.3150       | 0.3157       | 0.3165       | 0.3098       | 3.3191        |
|          | $\omega$ | 597.78       | 597.25       | 597.25       | 599.39       | 596.18        |
| 2        | <i>B</i> | 0.3155       | 0.3150       | 0.3151       | 0.3117       | 0.3155        |
|          | $\omega$ | 597.78       | 597.78       | 597.25       | 599.39       | 596.18        |
| 3        | <i>B</i> | 0.3151       | 0.3141       | 0.3144       | 0.3142       | 0.3155        |
|          | $\omega$ | 598.32       | 597.78       | 597.78       | 599.39       | 596.71        |
| 4        | <i>B</i> | 0.3144       | 0.3135       | 0.3129       | 0.3156       | 0.3119        |
|          | $\omega$ | 597.78       | 597.78       | 597.78       | 598.85       | 597.25        |
| 5        | <i>B</i> | 0.3136       | 0.3128       | 0.3117       | 0.3190       | 0.3106        |
|          | $\omega$ | 597.78       | 598.32       | 598.32       | 598.32       | 597.25        |
| 6        | <i>B</i> | 0.3144       | 0.3116       | 0.3115       | 0.3217       | 0.3098        |
|          | $\omega$ | 597.78       | 598.32       | 598.32       | 597.25       | 598.32        |
| 7        | <i>B</i> | —            | 0.3132       | 0.3118       | 0.3232       | 0.3094        |
|          | $\omega$ | —            | 598.85       | 598.85       | 596.18       | 598.32        |
| 8        | <i>B</i> | —            | —            | 0.3119       | 0.3241       | 0.3100        |
|          | $\omega$ | —            | —            | 598.32       | 595.65       | 598.85        |
| 9        | <i>B</i> | —            | —            | —            | 0.3230       | 0.3108        |
|          | $\omega$ | —            | —            | —            | 595.12       | 599.39        |
| 10       | <i>B</i> | —            | —            | —            | —            | 0.3115        |
|          | $\omega$ | —            | —            | —            | —            | 599.39        |



a) Odd number liquid slugs



b) Even number liquid slugs

Fig. 11 Displacement of liquid slugs ( $\varepsilon = 0.45$ ).

Figure 7 shows the dimensionless displacements of liquid slugs for a PHP with 10 turns after steady oscillation is established. The phases of oscillation for all odd-numbered liquid slugs are very close to each other, and the phases of oscillation for all even-numbered liquid slugs are also very close to each other. The phase difference between any two adjacent liquid slugs is approximately  $\pi$ . Figure 8 shows the overall displacements of liquid slugs at four different times.

The oscillations of any two adjacent liquid slugs are nearly always in opposing directions. The delay of oscillation for the  $i$ th slug relative to the  $(i - 2)$ th slug is also clearly seen from Fig. 8. Figure 9 shows the displacements of liquid slugs for  $L_h^* = L_c^* = 0.45$ . The overall distribution of the displacements of liquid slugs at four different times is shown in Fig. 10. The delay of oscillation for the  $i$ th slug relative to the  $(i - 2)$ th slug is more significant when the lengths of the heating and cooling sections are reduced. The amplitude and circular frequency of oscillation are listed in Table 2. Both the amplitude and circular frequency of oscillation are decreased

Table 2 Effects of heating/cooling section length and charge ratio on amplitude and circular frequency

| <i>i</i> |          | $L_h^* = 0.5$<br>$\varepsilon = 0.4$ | $L_h^* = 0.45$<br>$\varepsilon = 0.4$ | $L_h^* = 0.5$<br>$\varepsilon = 0.45$ |
|----------|----------|--------------------------------------|---------------------------------------|---------------------------------------|
| 1        | <i>B</i> | 0.3191                               | 0.3187                                | 0.2816                                |
|          | $\omega$ | 596.18                               | 581.65                                | 638.32                                |
| 2        | <i>B</i> | 0.3155                               | 0.3141                                | 0.2807                                |
|          | $\omega$ | 596.18                               | 582.16                                | 638.93                                |
| 3        | <i>B</i> | 0.3135                               | 0.3088                                | 0.2803                                |
|          | $\omega$ | 596.71                               | 582.67                                | 638.93                                |
| 4        | <i>B</i> | 0.3119                               | 0.3052                                | 0.2796                                |
|          | $\omega$ | 597.25                               | 583.17                                | 639.54                                |
| 5        | <i>B</i> | 0.3106                               | 0.3044                                | 0.2792                                |
|          | $\omega$ | 597.25                               | 583.68                                | 638.93                                |
| 6        | <i>B</i> | 0.3098                               | 0.3044                                | 0.2789                                |
|          | $\omega$ | 598.32                               | 584.19                                | 639.54                                |
| 7        | <i>B</i> | 0.3094                               | 0.3044                                | 0.2790                                |
|          | $\omega$ | 598.32                               | 584.71                                | 639.54                                |
| 8        | <i>B</i> | 0.3100                               | 0.3055                                | 0.2797                                |
|          | $\omega$ | 598.85                               | 584.71                                | 639.54                                |
| 9        | <i>B</i> | 0.3108                               | 0.3064                                | 0.2797                                |
|          | $\omega$ | 599.39                               | 585.22                                | 639.54                                |
| 10       | <i>B</i> | 0.3115                               | 0.3071                                | 0.2787                                |
|          | $\omega$ | 599.39                               | 585.22                                | 639.54                                |

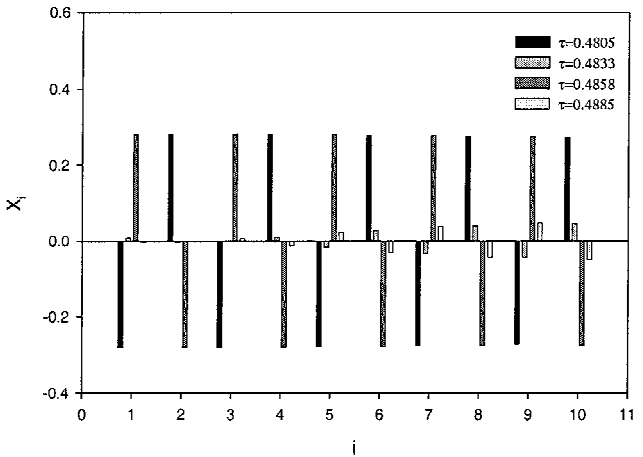


Fig. 12 Distribution of the displacement of liquid slugs ( $\varepsilon = 0.45$ ).

because the available heating and cooling section areas are decreased. Figure 11 shows the displacements of liquid slugs for the charge ratio of 0.45. The overall distribution of the displacements of liquid slugs at four different times is shown in Fig. 12. The oscillations of the  $i$ th slug relative to the  $(i - 2)$ th slug are closer to one another. The amplitude and circular frequency of oscillation for an increased charge ratio are also listed in Table 2. The amplitude of oscillation is decreased because the mass of the liquid slug is larger for a large charge ratio. On the other hand, the circular frequency of oscillation is increased.

### Conclusions

Oscillatory flow in a PHP with an arbitrary number of turns is investigated in the present study. The governing equations that describe the oscillatory flow were nondimensionalized, and the parameters that describe the system were reduced to eight nondimensional parameters. The results show that the increase in the number of turns has no effect on the amplitude and circular frequency of oscillation when the number of turns is less than or equal to five. When the number of turns is increased to more than five, the amplitude and circular frequency of oscillation for different liquid slugs are shown. Both the amplitude and circular frequency of oscillation will decrease when the lengths of the heating and cooling sections are decreased. When the charge ratio is increased, the amplitudes of oscillation decrease, and the circular frequency of oscillation increases.

### Acknowledgments

This work was partially supported by NASA Grant NAG3-1870 and National Science Foundation Grant CTS 9706706.

### References

- <sup>1</sup>Akachi, H., "Looped Capillary Heat Pipe," Japanese Patent No. Hei6-97147, 1994.
- <sup>2</sup>Faghri, A., *Heat Pipe Science and Technology*, Taylor and Francis, Washington, DC, 1995.
- <sup>3</sup>Akachi, H., Polasek, F., and Stulc, P., "Pulsating Heat Pipes," *Proceedings of the 5th International Heat Pipe Symposium*, Royal Melbourne Inst. of Technology, Melbourne, Australia, 1996, pp. 208–217.
- <sup>4</sup>Gi, K., Maezawa, K. Y., and Yamazaki, N., "CPU Cooling of Notebook PC by Oscillating Heat Pipe," *Proceedings of the 11th International Heat Pipe Conference*, Japan Association for Heat Pipes, Tokyo, Japan, 1999, pp. 166–169.
- <sup>5</sup>Miyazaki, Y., and Akachi, H., "Heat Transfer Characteristics of Looped Capillary Heat Pipe," *Proceedings of the 5th International Heat Pipe Symposium*, Royal Melbourne Inst. of Technology, Melbourne, Australia, 1996, pp. 378–383.
- <sup>6</sup>Miyazaki, Y., and Akachi, H., "Self Excited Oscillation of Slug Flow in a Micro Channel," *Proceedings of the 3rd International Conference on Multiphase Flow*, Lyon, France, 1998.
- <sup>7</sup>Miyazaki, Y., and Arikawa, M., "Oscillatory Flow in the Oscillating Heat Pipe," *Proceedings of the 11th International Heat Pipe Conference*, Japan Association for Heat Pipes, Tokyo, Japan, 1999, pp. 131–136.
- <sup>8</sup>Lee, W. H., Jung, H. S., Kim, J. H., and Kim, J. S., "Flow Visualization of Oscillating Capillary Tube Heat Pipe," *Proceedings of the 11th International Heat Pipe Conference*, Japan Association for Heat Pipes, Tokyo, Japan, 1999, pp. 131–136.
- <sup>9</sup>Hosoda, M., Nishio, S., and Shirakashi, R., "Meandering Closed-Loop Heat-Transport Tube (Propagation Phenomena of Vapor Plug)," *Proceedings of the 5th ASME/JSME Joint Thermal Engineering Conference*, American Society of Mechanical Engineers, New York, 1999 [CD-ROM].
- <sup>10</sup>Shafii, M. B., Faghri, A., and Zhang, Y., "Thermal Modeling of Unlooped and Looped Pulsating Heat Pipes," *Journal of Heat Transfer*, Vol. 123, No. 6, 2001, pp. 1159–1172.
- <sup>11</sup>Zhang, Y., Faghri, A., and Shafii, M. B., "Analysis of Liquid–Vapor Pulsating Flow in a U-Shaped Miniature Tube," *International Journal of Heat and Mass Transfer*, Vol. 45, No. 12, 2002, pp. 2501–2508.
- <sup>12</sup>Zhang, Y., and Faghri, A., "Heat Transfer in a Pulsating Heat Pipe with Open End," *International Journal of Heat and Mass Transfer*, Vol. 45, No. 4, 2002, pp. 755–764.